ORIGINAL PAPER

Food dyes screening using electrochemistry approach in solid state: the case of sunset yellow dye electrochemical behavior

Ana Maria Munaretto Durigon[1] · Géssica Domingos da Silveira[2] · Flávio Roberto Sokal[1] ·
Roni Anderson Capa Verde Pires[1] · Daiane Dias[1]

Abstract

Concerning the importance of the identification and characterization of food dyes in food science, this work presents a screening method using voltammetry of immobilized microparticles for identification in solid state of sunset yellow, tartrazine yellow, brilliant blue, indigotine, and erythrosine in food matrices. Different aqueous supporting electrolyte were investigated for screening purpose and NaCl 0.1 mol L^{-1} showed to be suitable for evaluating dyes in solid state. By using square wave voltammetry as detection mode was possible to establish qualitative diagnostic criteria for identification of dyes in commercials powder of food dyes samples using both anodic and cathodic scan. Moreover, based on the solid-state electrochemistry profile and due to the lack of information about the electrochemical behavior of these compounds in solid state, some oxi/reduction pathways could be elucidated, and special attention was given to the case of sunset yellow dye.

Keywords Electrochemical pathways · Food dyes · Screening · Solid state · Sunset yellow · voltammetry

Introduction

The fast development of the food industry has led to the intense use and incorporation of food additives, such as preservatives, sweeteners, thickeners, and dyes, which are used to guarantee and improve the organoleptic properties of foods [1]. Dyes are extremely relevant because food quality and flavor are often associated with colors [2]. However, synthetic dyes do not provide any nutrients and may even endanger human health by causing allergies, thyroid activities, respiratory and gastric problems, hyperactivity in children and even carcinogenic effects, DNA damage, and neurotoxicity [3].

✉ Daiane Dias
   daianezd@gmail.com

1   Laboratório de Eletro-Espectro Analítica (LEEA), Escola de Química e Alimentos, Universidade Federal do Rio Grande, Av. Itália km 8, 96203-900, Rio Grande, RS, Brazil

2   Institute of Chemistry, State University of Campinas, Rua Josué de Castro 126 Cidade Universitária, Campinas, SP 130810361, Brazil

The current European legislation allows (with the respective maximum concentration) the use of 11 artificial dyes (erythrosine, amaranth, azorubine, ponceau 4R, sunset yellow, tartrazine yellow, indigotine, brilliant blue, fast green and patent blue V) in foods and beverages with their compounds description in the marketed product [4]. Similar context is observed in some Latin American countries, such as Brazil where 11 artificial dyes (erythrosine, amaranth, azorubine, ponceau 4R, sunset yellow, red 40, tartrazine yellow, indigotine, brilliant blue, fast green and blue patent V) are allowed in foods and beverages with the compounds description in the marketed product [5]. On the other hand, the USA legislation prohibits the use of 4 dyes (amaranth, ponceau 4R, azorubine, and patent blue V) often used in foods in Brazil and Europe Union [6]. In consequence, any food containing a substance not approved by the legislation is considered adulterated and is subject to coercive measures to have it removed from trade [7].

Hence, to meet the requirements for food safety, analytical methods have been proposed towards the identification and characterization of synthetic food dyes, being liquid chromatography the preferred technique for those purpose [8, 9]. However, sample preparation for this kind of analysis is often necessary, since other substances contained in foods can be interfering or impairing the dye determinations. Besides the

fact that sample preparation step has been considered a source of errors [10], the cost of chromatographic analysis is higher than others, such as electrochemical techniques, mainly because of the high cost of equipment, maintenance, and high consumption of reagents.

Thus, electrochemical techniques emerges as an alternative analytical tool for determination of such compounds [3], especially because of the functional groups in their structures which could generate several oxidation/reduction signals that

can be used to characterization and determination of these compounds [11, 12]. Among the electrochemical methods available, voltammetry of immobilized microparticles (VIMPs) developed by Scholz and co-workers allows the electrochemical and electroanalytical information of samples in solid state [12–14]. This technique has demonstrated excellent results when applied to solid-state electrochemistry of pharmacological substances, organosulfur compounds, and organic dyes [11, 15–25]. The term screening can be applied

Table 1 Chemical structure and classes of food dyes used in this work

Dyes	Class	Chemical Structures
Sunset Yellow	Azo	
Tartrazine Yellow	Azo	
Erythrosine	Xanthene	
Indigotine	Indigoid	
Brilliant Blue	triphenylmethane	

Table 2 Anodic potential peaks (± 50 mV) of the compounds in HCl 0.1 mol L^{-1}. Square wave voltammetric parameters: E_{begin} − 0.6 V, E_{final} 1.3 V, E_{step} 4 mV, frequency 5 Hz, and amplitude 25 mV

Food dye	E_{pa1} (V)	E_{pa2} (V)	E_{pa3} (V)	E_{pa4} (V)	E_{pa5} (V)	E_{pa6} (V)
Sunset yellow	− 0.90	− 0.42	− 0.12	+ 0.18	+ 0.47	+ 1.00
Tartrazine yellow	− 0.90	− 0.41	− 0.09	+ 0.32	+ 0.51	+ 0.92
Erythrosine	− 0.75	+ 0.40	+ 0.09	+ 0.46	+ 0.80	+ 1.14
Indigotine	− 0.90	+ 0.03	+ 0.30	+ 0.51	+ 0.75	+ 1.15
Brilliant blue	− 0.75	− 0.35	+ 0.09	+ 0.42	+ 0.67	+ 1.01

to any analysis that produces as a result a set of signals capable of characterize a certain analyte (or analytes family) within a given matrix, where interferents may be present [19].

In this way, the present work aims to propose a screening method using VIMP for identification and characterization of food dyes in solid state in food matrices without prior sample preparation. Moreover, in view of the lack of information about the electrochemical behavior of such compounds in solid state, we aim to contribute with the oxi/reduction mechanism elucidation of sunset yellow dye in solid state. This compound was chosen since it belongs to the azo dye class that is widely used for food production in the world. Additionally, it is important to emphasize that in the literature up to date, no electrochemical studies have been found that can simultaneously characterize five food dyes (sunset yellow, tartrazine yellow, brilliant blue, indigotine, and erythrosine) without prior sample preparation or the use of multivariate tools.

Experimental

Chemicals and samples

The food dye standards (95% purity) sunset yellow, tartrazine yellow, brilliant blue, indigotine, and erythrosine (Duas Rodas, Brazil) were used in this work. The structural formulas of each dye are shown in Table 1. NaOH was purchased by Merck (Germany), and NaCl and HCl by Synth (Brazil). All solutions were prepared in ultrapure water (Millipore, Germany) with a resistivity of 18.2 MΩ cm^{-1}.

The samples used in this work were powder culinary dyes in yellow, blue, green, black, and red colors (Regina Ind. and Com. SA, Brazil) purchased from local market in Rio Grande, RS.

Voltammetry of immobilized microparticles

Voltammetric analyses were performed using a Multi Potentiostat/Galvanostat M204 (Autolab, Netherlands) controlled by Nova 2.1.4 software (Eco Chemie). The data for all measurements were processed using Origin Pro 8.0 program.

Three electrodes constituted the electrochemical cell: a graphite bar (2-mm diameter cylindrical rods, OF/9020HB, Faber Castell, Brazil) was used as working electrode, an Ag/AgCl (KCl 3 mol L^{-1}) as reference electrode and platinum as the auxiliary electrode.

To evaluate the electrochemical profile of the compounds, square wave voltammetry (SWV) was used with 4 mV E_{step}, 25-mV amplitude, and 5-Hz frequency with potentials from − 0.6 to 1.3 V (for HCl), − 1.2 to 0.9 V (for NaOH), and − 1.2 to 1.2 V (for NaCl). The influence of the electrolyte composition (NaOH, HCl, and NaCl) and concentration (0.1 and 1 mol L^{-1}) was evaluated by SWV. In addition, anodic and cathodic cyclic voltammetry (CV) analyses were performed, starting at

Fig. 1 Summary representation of the screening voltammetric profile of the solid compounds using HCl 0.1 mol L^{-1} for VIMP measurements
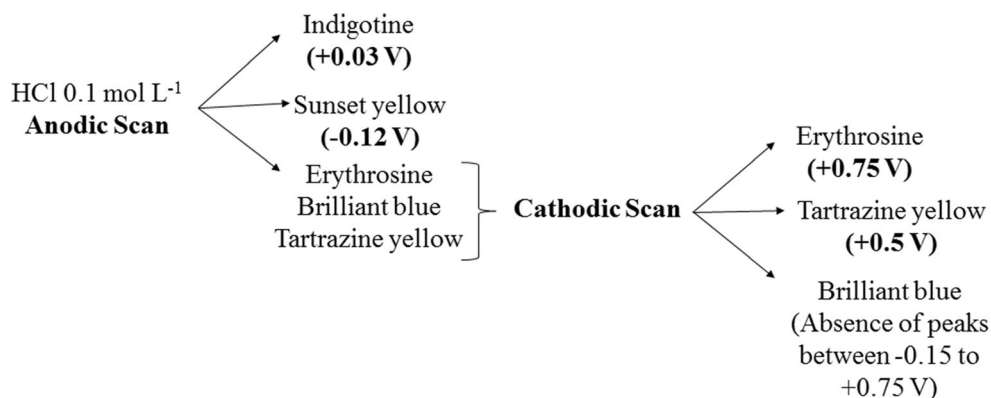
Table 3 Anodic potential peaks (± 50 mV) of the compounds in NaOH 0.1 mol L^{-1}. Square wave voltammetric parameters: E_{begin} − 1.2 V, E_{final} 0.9 V, E_{step} 4 mV, frequency 5 Hz, and amplitude 25 mV

Food dye	E_{pa1} (V)	E_{pa2} (V)	E_{pa3} (V)	E_{pa4} (V)	E_{pa5} (V)	E_{pa6} (V)	E_{pa7} (V)	E_{pa8}(V)
Sunset yellow	− 0.90	− 0.60	− 0.44	− 0.19	+ 0.02	+ 0.24	+ 0.48	+ 0.71
Tartrazine yellow	− 0.94	− 0.63	− 0.24	+ 0.12	+ 0.23	+ 0.47	+ 0.66	+ 0.87
Erythrosine	− 0.93	− 0.63	− 0.48	− 0.26	− 0.01	+ 0.72	+ 0.80	
Indigotine	− 0.53	+ 0.03	+ 0.41	+ 0.82				
Brilliant blue	− 0.70	− 0.44	− 0.04	+ 0.55				

0.25 V (1.4 to − 1.4 V), with 50 mV s^{-1} and 44 mV for potential step.

In the case of voltammetric analyses in solution phase, 2 mg L^{-1} of sunset yellow dye and NaCl 0.1 mol L^{-1} as supporting electrolyte were used for performing the measurements by CV in anodic and cathodic directions starting at 0.25 V (1.4 at − 1.4 V) using 50 mV s^{-1} and 44 mV for step potential.

For solid compound immobilization in the working electrode, first the maceration of the standards and samples (culinary dyes) were carried out with an agate mortar and pistil, to ensure the uniformity of the particles and also to obtain the finely distributed material. The graphite electrode was pressed on the sample to immobilize the solid compounds by abrasion. Afterwards, the electrode was carefully added to the voltammetric cell, and only the electrode surface containing the particles immobilized was in contact with the supporting electrolyte.

All voltammograms generated for the standards and samples were discounted to the response of the graphite electrode without immobilization, to eliminate the contribution of blank's response. This discount was made using Nova 2.1.4 software.

Fourier transform infrared spectroscopy and Scanning electron microscopy

Fourier transform infrared spectroscopy (FTIR, IR PRESTIGE-21 model, Shimadzu, Japan) was used to obtain spectra of the oxidation/reduction products. The graphite with the immobilized compound was subjected to electrolysis at

fixed potentials (+ 1.3 or − 1.3 V) for 30 s in contact with NaCl 0.1 mol L^{-1}. After the solvent evaporation, the material was removed from the graphite by scraping and it was mixed and macerated with potassium bromide. The analyses were carried out from 4000 to 400 cm^{-1} with 4 cm^{-1} resolution using the diffuse reflectance method.

For the morphological analyses, Dentun Vacuum equipment and a scanning electron microscope (SEM) JSM 6610 LV (JEOL, Japan) were used, operating at 20 kV. For this, the graphite electrodes containing the sunset yellow dye immobilized obtained by electrolysis under fixed potentials (+ 1.3 or −1.3 V) for 30 s in contact with NaCl 0.1 mol L^{-1} were fixed in a stub using double-sided adhesive tape and then these were coated with gold for 300 s at a current of 50 mA.

Results and discussion

Food dye voltammetric response in solid state: qualitative diagnostic criteria for discrimination

Food dyes sunset yellow, tartrazine yellow, erythrosine, indigotine, and brilliant blue were individually immobilized in a graphite working electrode surface and voltammograms (Online resource 1 to 5, respectively) were obtained by SWV in HCl, NaOH and NaCl 0.1 mol L^{-1}. As it can be observed, all compounds presented well-defined voltammetric response with several anodic and cathodic peaks due to the functional groups in their structures that can easily undergo electrochemical processes in solid-state. The choice of the best supporting

Fig. 2 Summary representation of the screening voltammetric profile of the solid compounds using NaOH 0.1 mol L^{-1} for VIMP measurements
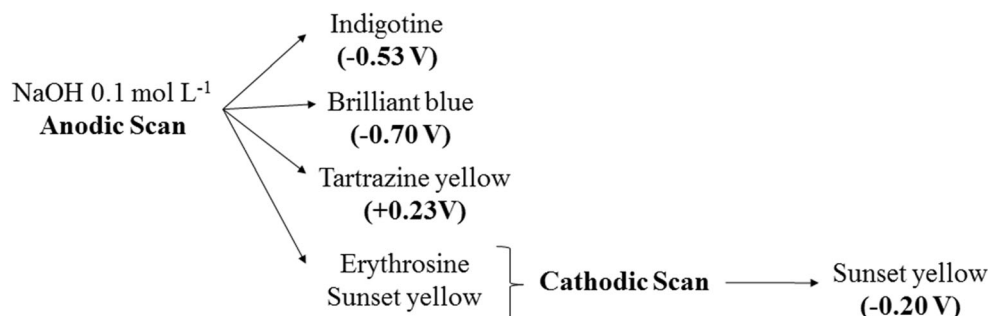
electrolyte was made by screening, seeking cleaner voltammograms with well-defined peaks that can support the distinction between the dyes.

Differences of the compounds response in the voltammetric are mainly associated to the features of immobilized microparticles electrochemical reaction, which according to the theory of Lovric and Scholz is assumed to undergo by insertion/de-insertion of cations and electron hopping [26] but also anion insertion/release process can occur [27] at the particle/electrolyte/electrode junction [15]. The
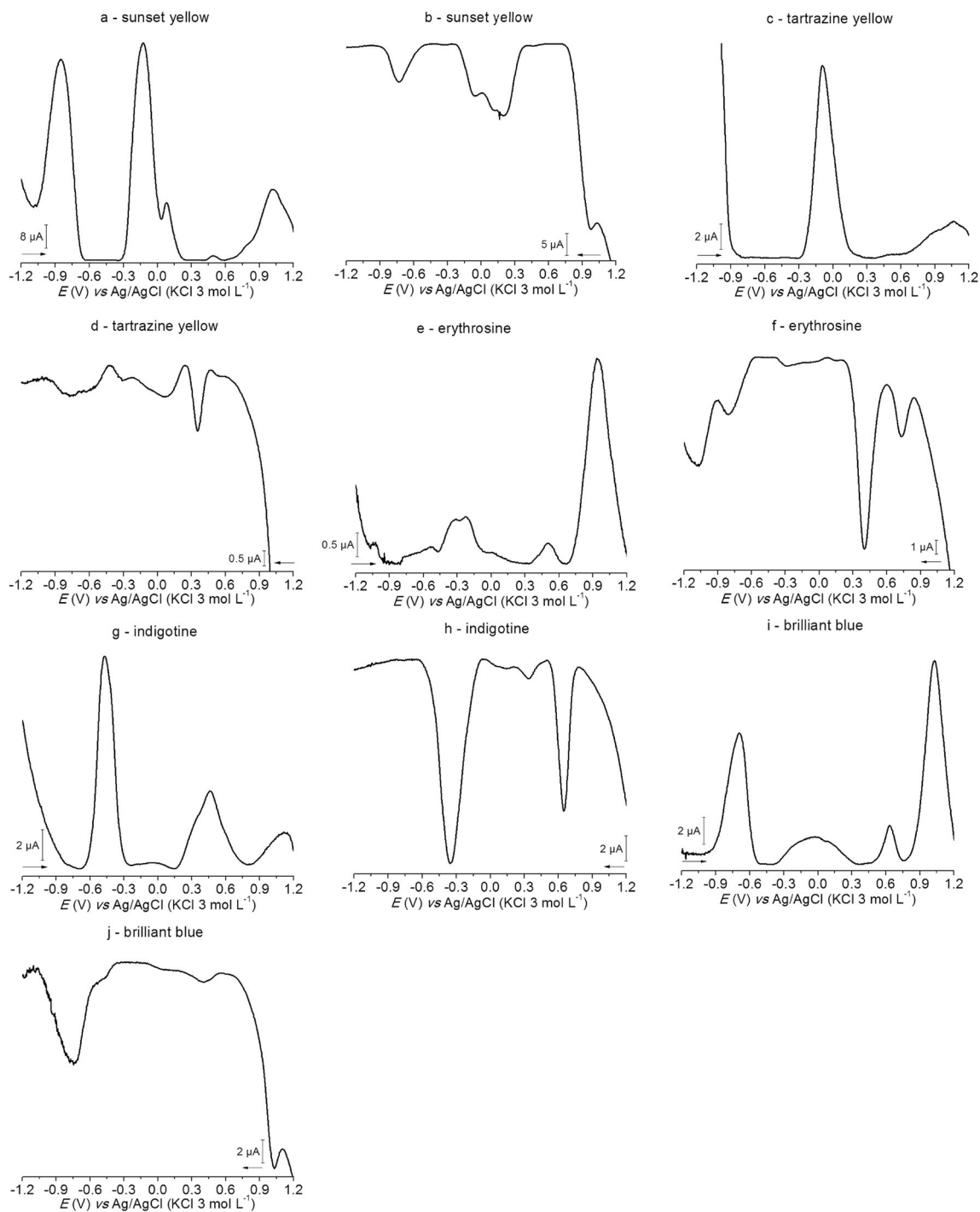
Fig. 3 Square wave voltammograms of **a** anodic and **b** cathodic scans of sunset yellow, **c** anodic and **d** cathodic scan of tartrazine yellow, **e** anodic and **f** cathodic scan of erythrosine, **g** anodic and **h** cathodic scan of indigotine, and **i** anodic and **j** cathodic scan of brilliant blue in solid state with the microparticles immobilized on the graphite electrode in NaCl 0.1 mol L^{-1} from − 1.2 to 1.2 V. Square wave voltammetric parameters: E_{step} 4 mV, frequency 5 Hz, and amplitude 25 mV

Table 4 Anodic potential peaks (± 50 mV) of the compounds in NaCl 0.1 mol L^{-1}. Square wave voltammetric parameters: E_{begin} − 1.2 V, E_{final} 1.2 V, E_{step} 4 mV, frequency 5 Hz, and amplitude 25 mV

| Food dye	E_{pa1} (V)	E_{pa2} (V)	E_{pa3} (V)	E_{pa4} (V)	E_{pa5} (V)	E_{pa6} (V)	E_{pa7} (V)
Sunset yellow	− 0.85	− 0.13	− 0.08	+ 0.1	+ 0.48	+ 0.77	+ 1.0
Tartrazine yellow	− 0.09	− 0.83	+ 1.05				
Erythrosine	− 1.02	− 0.53	− 0.34	− 0.20	+ 0.016	+ 0.50	+ 0.94
Indigotine	− 0.46	− 0.06	+ 0.31	+ 0.46	+ 1.1		
Brilliant blue	− 0.70	− 0.05	+ 0.63	+ 1.02			

theoretical aspects for organic compounds electrochemical re-action in solid state using VIMP have been addressed in the literature [27–31] and different cations and anions of the elec-trolyte can lead to different voltammetric response of the com-pounds. Discussion about the theoretical aspects will be out of scope in this work.

Upon scanning the potential from − 0.6 to 1.3 V, several anodic peaks were recorded using HCl 0.1 mol L^{-1} (Online resource 1 to 5). The main anodic potential peaks (E_{pa}) of the compounds are presented and compared in Table 2. It is pos-sible to observe that only indigotine and sunset yellow pre-sented distinct peaks that could be used for screening purpose at around + 0.03 (E_{pa2}) and − 0.12 V (E_{pa3}), respectively. Additionally, erythrosine, brilliant blue and tartrazine yellow presented overlapping peaks in the positive potential region and they could not be distinguished from each other during anodic scan.

When backward scan was performed, erythrosine and tartrazine yellow presented cathodic signals at around + 0.75 V and + 0.5 V, respectively, while other compounds presented overlapping cathodic peaks. As showed in Fig. 1, brilliant blue could be distinguished in the cathodic scan by absence of cathodic processes from − 0.15 to + 0.75 V. The compounds screening voltammetric profile in HCl 0.1 mol L^{-1} are summarized in Fig. 1 and as it can be observed is possible to identify indigotine and sunset yellow in anodic scan, as well as to confirm the presence of erythrosine, tartrazine yellow and brilliant blue in cathodic scan (not pos-sible in anodic scan).

In the same way, NaOH 0.1 mol L^{-1} was tested as supporting electrolyte and several anodic peaks were observed for the compounds as depicted in Online resource 1 to 5. This electrolyte presented a background current higher than HCl or NaCl, and it was also considered a negative parameter to use

Fig. 4 Summary representation of the screening voltammetric profile of the solid compounds using NaCl 0.1 mol L^{-1} for VIMP measurements
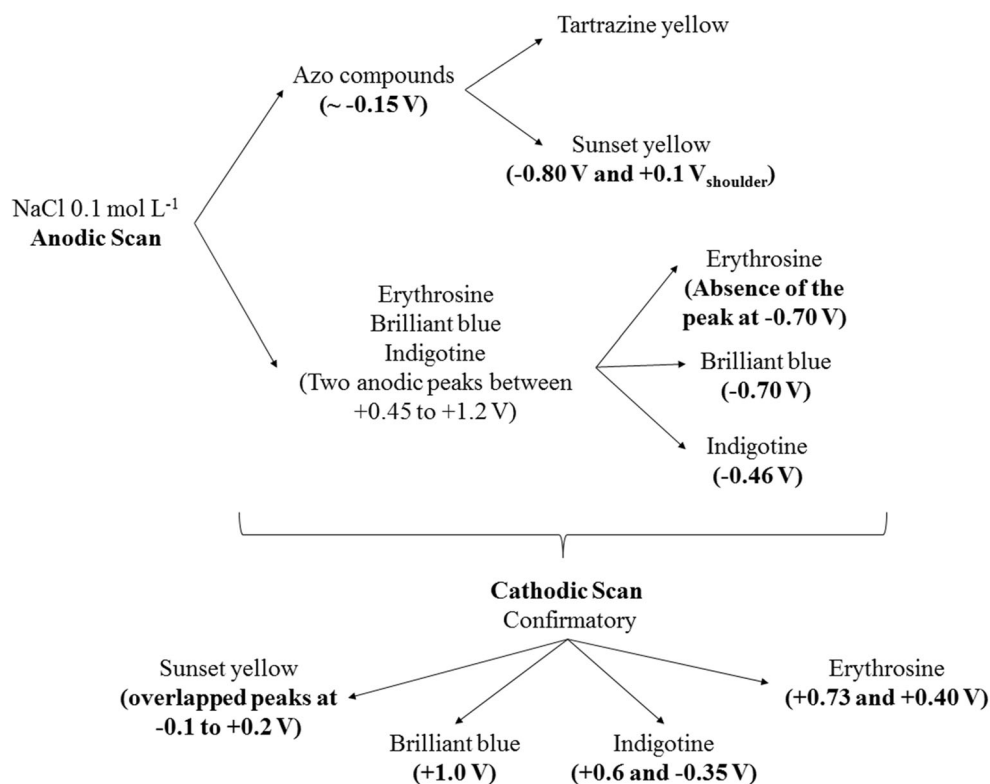
NaOH for screening purpose, since the peaks in the voltammogram, after the discount of the blank, could result in a misleading interpretation of the results. Moreover, as it can be observed, the voltammograms present anodic and cathodic signal, which turns the discrimination of the dyes more difficult without a multivariate analysis. Voltammetric profile in alkaline media changes significantly for compounds, such as indigotine and it can be associated to the higher solubility of the redox products as already reported for indigo-based dyes [32, 33].

Upon scanning the potential in the positive direction, the dyes indigotine, brilliant blue, and tartrazine yellow present remarkable anodic peaks at around -0.53 (E_{pa1}), -0.70 (E_{pa1}), and $+0.23$ V (E_{pa5})respectively, which are shown in Table 3. Additionally, erythrosine and sunset yellow presented overlapping peaks in the anodic scan making their distinction difficult. However, even in the backward scan, it was not possible to distinguish the five dyes by using NaOH 0.1 mol L^{-1}. Figure 2 summarizes the main peaks differences among the compounds and the grouping observed by overlapped processes during anodic and cathodic scan. As it can be observed in NaOH, it is possible to identify indigotine, brilliant blue, and tartrazine yellow in anodic scan, as well as to confirm the presence of sunset yellow in cathodic scan (not possible in anodic scan).

The food dyes' voltammetric response were also evaluated using NaCl 0.1 mol L^{-1} as supporting electrolyte for VIMP measurements, and the voltammograms obtained for both anodic and cathodic scan are depicted in Fig. 3.

Comparing these results with those from Online resource 1 to 5, it is possible to observe that the voltammograms obtained in NaCl were cleaner than in HCl or NaOH; less anodic and cathodic processes were observed as it will be discussed in the following. Moreover, the background current was lower, leading to stable voltammetric response of the solid compounds. The absence of many peaks in NaCl 0.1 mol L^{-1} could be associated to the less solubility of the solid dyes and its oxidation/reduction products in the supporting electrolyte. Related to this same examples can be highlighted such as the presence of (i) cathodic peaks at 0.3 and 0.45 V for sunset yellow in HCl and NaOH, respectively; (ii) some anodic peaks from -1.2 to -0.3 V and from 0.2 to 0.8 V in the voltammograms for tartrazine yellow in NaOH as well as at 0.32 V in HCl; (iii) an anodic peak at 0.03 V and an overlap cathodic peaks from around 0.15 to -0.25 V for indigotine in HCl and NaOH; (iv) an anodic peak at -0.4 V in HCl and NaOH for brilliant blue. Compound solubility can influence in the voltammetric response of the solid analytes immobilized into electrode, mainly because sparingly soluble species can undergo solution electrochemical reactions. This can be a problem in VIMP with screening purpose, since the solution reaction occurs simultaneously to electrochemical reaction in solid

state leading to additional peaks in the voltammograms and even overlapping solid-state processes.

As depicted in anodic scans shown in Fig. 3a, c and Table 4, upon scanning the potential in the positive direction, the azo compounds sunset yellow and tartrazine yellow presented an intense anodic peak from -0.30 to 0.15 V (E_{pa3} and E_{pa1} in the case of sunset yellow and tartrazine yellow, respectively). Additionally, it is possible to observe other anodic peak around $+1.0$ V (E_{pa7} and E_{pa3} in the case of sunset yellow and tartrazine yellow, respectively) possibly derived from an oxidation of hydroxyl to carbonyl groups. Sunset yellow even presented an intense anodic peak at around -0.85 V and a shoulder at around 0.1 V (E_{pa1} and E_{pa4}, respectively), which will be discussed forward. Table 4 compares the anodic peaks mapped for all compounds.
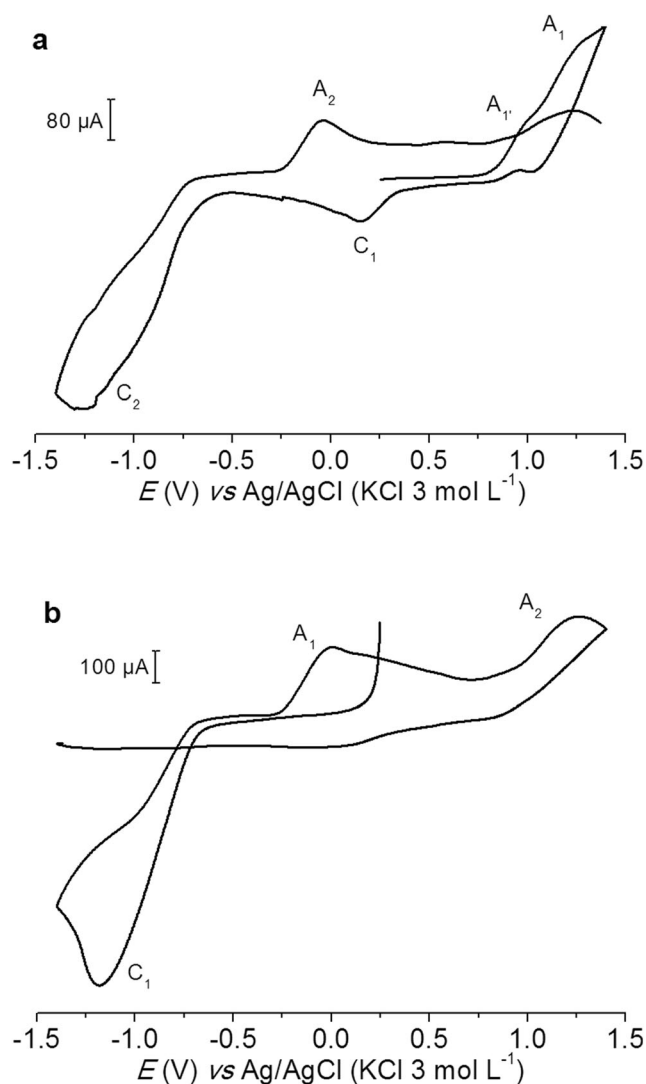
Fig. 5 Anodic (**a**) and cathodic (**b**) cyclic voltammograms of sunset yellow microparticles immobilized on the graphite electrode in NaCl 0.1 mol L^{-1} from -1.4 to 1.4 V (start potential of 0.25 V) with scan rate of 50 mV s^{-1}
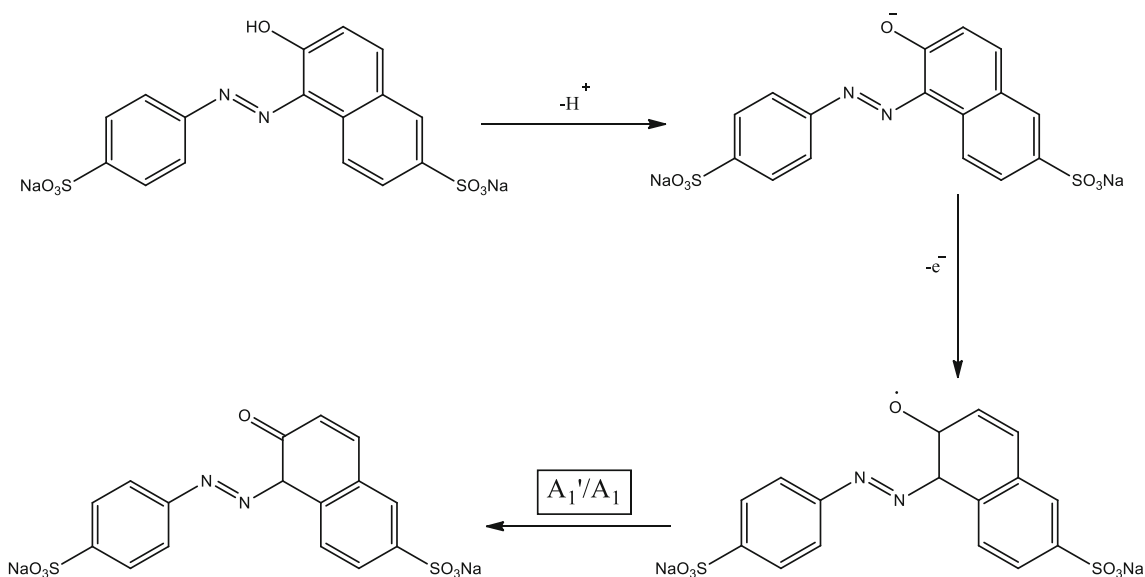
Scheme 1 Steps in the oxidation of hydroxyl group in the sunset yellow structure during CV anodic scan

As observed in Table 4, erythrosine (Fig. 3e) and brilliant blue (Fig. 3i) presented two anodic peaks between + 0.45 and + 1.2 V (E_{pa6} and E_{pa7} in the case of erythrosine at + 0.50 and + 0.94 V, respectively, as well as E_{pa3} and E_{pa4} in the case of brilliant blue at + 0.63 and + 1.02 V, respectively); however, brilliant blue presented an intense anodic peak at around − 0.70 V (E_{pa1}) which could be used for discrimination of these dyes. Indigotine also presented peaks between + 0.45 and + 1.2 V (E_{pa4} and E_{pa5} at + 0.46 and + 1.1 V, respectively), but its anodic discrimination related to indigotine (Fig. 3g) and brilliant blue was possible due to electrochemical process of indigotine at − 0.46 V (E_{pa1}), not present in brilliant blue voltammogram.

During the backward scan, the dyes also presented characteristic peaks that can be used for screening purpose, as it can be on the cathodic scans observed in Fig. 3. In the negative direction, brilliant blue (Fig. 3j) presents a confirmatory cathodic peak at around + 1.0 V and indigotine (Fig. 3h) presents two characteristic processes at + 0.6 and − 0.35 V. Erythrosine (Fig. 3f) presented a cathodic peak at + 0.73 V followed by an intense peak at + 0.40 V and two peaks in more negative regions (− 0.8 and − 1.1 V). Moreover, sunset yellow (Fig 3b) can be confirmed during cathodic scan by the presence of three intense overlapped peaks at around + 0.4 to − 0.15 V.

Figure 4 summarizes the main anodic and cathodic processes that can characterize and confirm the food dyes presence in solid state.

As it can be observed, the use of NaCl 0.1 mol L^{-1} allowed the discrimination of the all food dyes under study in the anodic scan (sunset yellow, tartrazine yellow, brilliant blue, indigotine, and erythrosine). Additionally, during cathodic scan, it was possible to confirm the presence of four compounds (sunset yellow, brilliant blue, indigotine, and erythrosine) being this electrolyte more appropriated for screening purpose.

Electrochemical behavior and solid-state mechanism: the case of sunset yellow

Azo compounds are one of the most used dyes class allowed in foods [34] and the solution electrochemistry of these compounds have been addressed in the literature [35, 36]. The reduction and oxidation reactions of these compounds in the working electrode surface occurs similarly in the metabolic processes; thus, the mechanistic studies are relevant [35]. Moreover, the electrochemical behavior of these compounds in solid state was not related in the literature so far we known and some electrochemical pathways could be identified in this work and they will be described in the following.
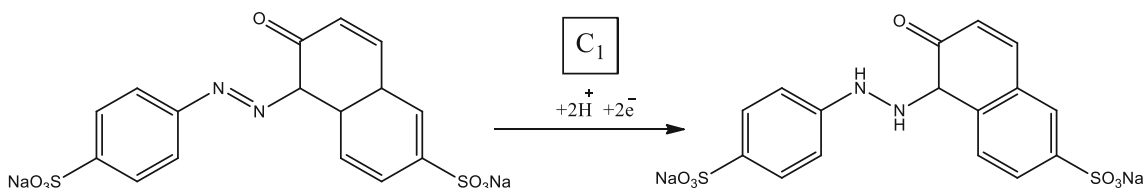
Scheme 2 Reduction of the nitrogen double bond to hydrazo during cathodic scan
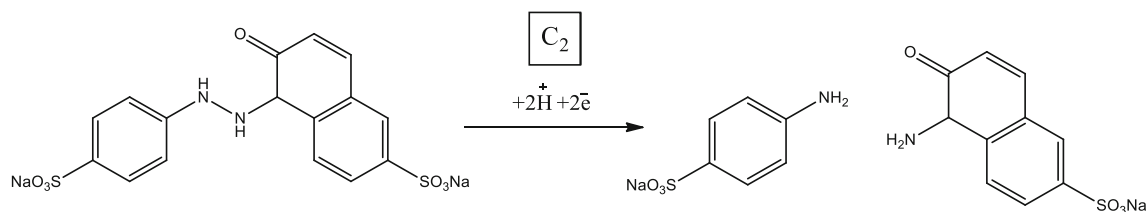
Scheme 3 Reduction of the nitrogen bond during cathodic scan forming the correspondent amine

In view of the electrochemical mechanisms complexity in solid state, azo compound cyclic voltammograms were recorded in both anodic and cathodic scan direction and the sunset yellow was chosen to elucidate the reaction mechanisms. Figure 5 a shows the cyclic voltammogram for dye upon scanning the potential in the positive direction. When compared to solution phase cyclic voltammograms (Online resource 6), solid-state electrochemical features were observed and based on that, some mechanisms were proposed.

As depicted in Fig. 5a, two oxidation processes were observed during anodic scan at around + 0.9 and + 1.2 V assigned as A_1' and A_1, respectively. During the backward scan, two cathodic processes were observed at around + 0.18 and − 1.4 V (C_1 and C_2, respectively) and following the scan up to end potential (+ 1.4 V), an anodic peak A_2 was observed at − 0.07 V.

The signals A_1 and A_1' were reasonably attributed to oxidation of the hydroxyl group bound to the aromatic ring in the ortho position to the azo bond [36], as described in Scheme 1:

The two oxidation peaks obtained in the first scan are related to (i) the radical formation phase of the carboxyl (A_1'), where firstly the loss of a proton occurs and after the loss of one electron, forming the double bond between the benzenic carbon and oxygen followed by (ii) the direct formation of the double bond between carbon and oxygen, generated from the simultaneous transfer of proton and electron involved in the reaction (A_1) [30]. Moreover, these signals were also present in solution phase cyclic voltammograms (Online resource 6) during anodic scan, thus inferring that the solid compounds undergo a dissolutive oxidation process.

According to the literature, the presence of an electron withdrawing group in ortho position to azo bond allows the partial reduction of the double bond between the nitrogens [35]. This occurs because the electron withdrawing group decreases the electron density between the nitrogens, favoring the breaking in stages of the double bound. In this way, upon scanning the potential in the negative direction, the cathodic

peak at around + 0.18 V (C_1) was attributed to the reduction of the azo bond to hydrazo due to the presence of the carboxyl (an electron withdrawing group) in the ortho position to the this bond. In tartrazine yellow, the same signal was observed and it was rationalized in terms of the presence of carboxyl group in the molecular structure of this dye. This cathodic process was purposed in Scheme 2:

The hydrazo bond formed can be still reduced in more negative potential regions [36] forming correspondent amines by breaking the nitrogen bond. This cathodic process can be observed at around − 1.25 V (C_2), and it is described by the mechanism in Scheme 3. During the backward anodic scan in Fig. 5a, the amines generated can be oxidized [37] in the A_2 processes, as demonstrated in Scheme 4.

Upon starting the cyclic voltammogram in the negative potential direction, as depicted in Fig. 5b, it was possible to observe a reduction processes at around − 1.2 V assigned as C_1. This process was considered as the reduction of the azo group directly to amines and the reaction is demonstrated in Scheme 5.

The same peak was observed for tartrazine yellow, and it is an indicative of the azo group presence. As reported in the literature, compounds containing azo bonds with hydroxyl group adjacent to the double bond between nitrogens are reduced directly producing corresponding amines, which are more likely to be oxidized in the backward scan following the process observed in A_1 [37]. Moreover, direct reduction of the azo group to amine group occurs due to the increase in the electronic density generated by an electron donor group in an ortho position, which facilitates the protonation of nitrogen, leading to the formation of two corresponding amines [38]. Furthermore, when compared the voltammogram depicted in Fig. 5b with the one in solution phase (Online resource 6), the cathodic process observed in C_1 occurs in more negative potentials and it seems to be a genuine solid-state process.

The hydroxyl bound to the ring in one of the amines generated by the broken of the azo group can be oxidized
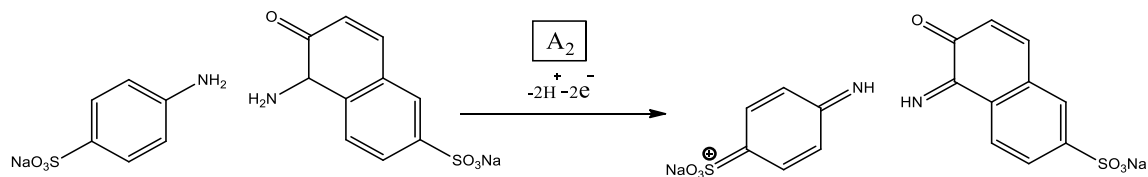
Scheme 4 Oxidation of the amines during backward scan
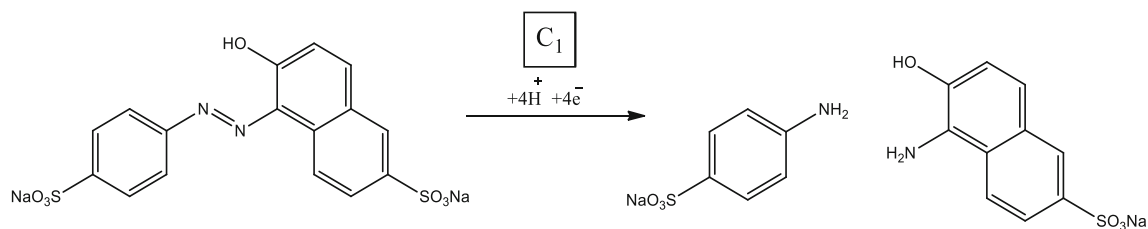
**Scheme 5** Reduction of the azo bond directly to corresponding amines

following the process in A_2 (Fig. 5b), and it is represented in Scheme 6:

The voltammogram profile depicted in Fig. 5b in more anodic potentials changed when compared to Fig. 5a, since this oxidation no longer involves a radical. Moreover, the absence of the cathodic peaks at around 0.20 and − 1.4 V in Fig. 5b is expected when compared to Fig. 5a, since the azo group is no longer present to form hydrazo groups, as previously proposed.

To confirm the mechanisms proposed, sunset yellow dye electrochemical behavior was investigated by FTIR (Figs. 6 and 7), and spectra were collected before and after the potential application in order to observe the changes during electrochemical processes. Once it is known that the formation of new products from solid compounds can also be observed by structural and morphological differences in the crystals immobilized onto the electrode surface [39], SEM images were also collected (before and after the potential application) to support the solid-state or solution phase nature of the electrochemical reactions (Online resource 7 to 9).

Figure 6 depicts the spectra of sunset yellow dye (a) before and (b) after the electrolysis under positive potential (+ 1.3 V) for 30 s. As it can be observed in Fig. 6a, the bands at 1240 and 1320 cm^{-1} assigned by an arrow are attributed to vibration of O-H and C-O-H bonds, respectively [40]. After electrochemical treatment (Fig. 6b), these bands presented several changes, such as decreasing intensity of the band at 1320 cm^{-1} or even disappearance of the peak, as assigned in 1240 cm^{-1}. These changes can be rationalized in terms of the hydroxyl groups oxidation after electrolysis, corroborating with voltammetric data and purposed mechanism depicted in Scheme 1.
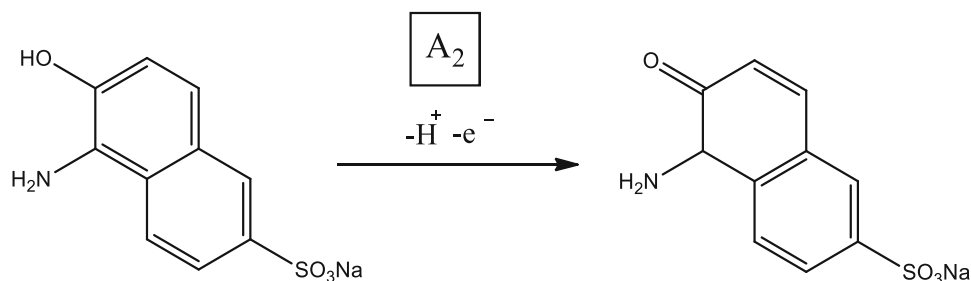
Moreover, when SEM images were collected after the electrolysis in positive potentials, the morphology of the crystals changed considerably as it can be observed in Online resource 7. Previously to the electrolysis (Online resource 8), the crystals present well-defined shapes and they were randomly distributed in the electrode surface. After the application of + 1.3 V during 30 s, the solid compound lost the defined shape and it seemed to suffer some erosion process. These features can be assigned as an oxidative dissolution of the hydroxyl group assisted by a de-insertion of the protons; thus, the solid compound generates a soluble product changing the crystalline pattern previously observed.

After electrolysis in negative potentials, sunset yellow demonstrated remarkable changes in the spectrum derived from reduction processes as depicted in Fig. 7.
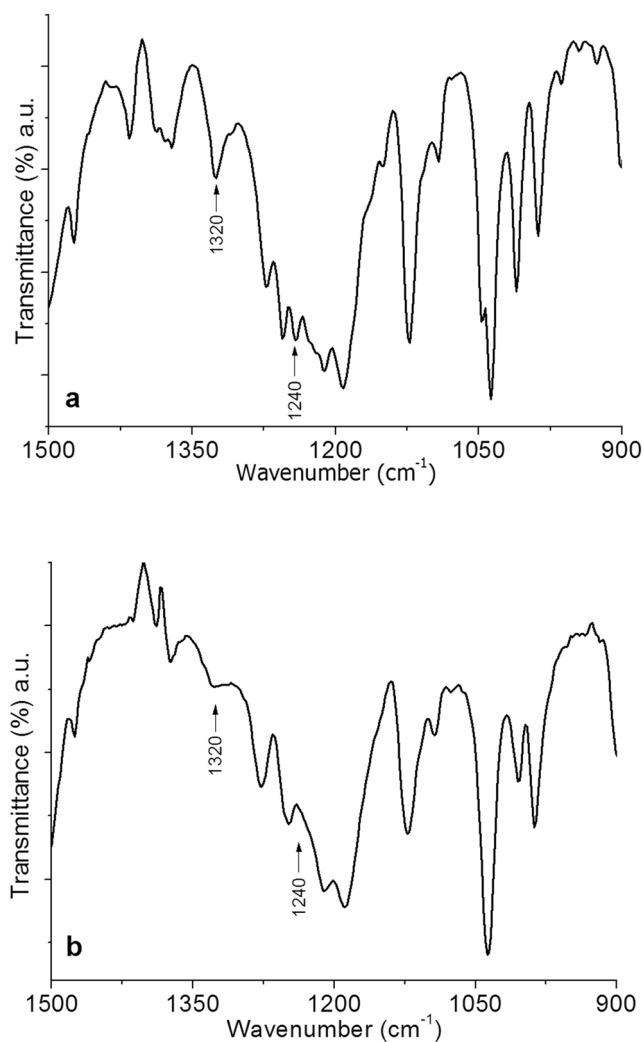
As it can be observed in Fig. 7b, after the electrolysis, there was a presence of a band at 1616 cm^{-1} characteristic of the N-H deformation bond in primary aromatic amines, and it was not present in the original spectrum (Fig. 7a). The emergence of this band can be attributed to the reduction of azo group in the sunset yellow during negative potentials forming N-H bonds, as suggested by the voltammetric data.

Moreover, SEM images collected after negative potential application demonstrated the formation of a new solid compounds in the crystals surface, suggesting that the reduction of the azo compounds can lead to solid reduction products, as can be observed in Online resource 9. The formation of these products on the crystal surface is in accordance with the theoretical aspects related to the VIMP electrochemical mechanism [26, 30], where the reaction occurs at the junction of the three phases forming products mainly in the vertices and on the crystal surface, involving two equilibria simultaneously

Scheme 6 Oxidation of the hydroxyl group during anodic scan

(ion exchange and charge transfer). Based on these results, it is possible that a solid-solid reduction assisted by protons insertion is occurring with the application of negative potentials, resulting in the formation of new solids on the crystal surface. Similar processes have recently been addressed for malachite green, organosulfur compounds, and some drugs, such as tadalafil [27, 39, 41].

Evaluation of real samples: Screening of commercial powder of food dyes

The presence of the five dyes under investigation was evaluated by the screening of commercial powder of food dyes using NaCl 0.1 mol L^{-1} for VIMP. Thus, based on the qualitative diagnostic criteria previously established, anodic and cathodic scans of the samples were performed to characterize and confirm the presence of the dyes in the samples.
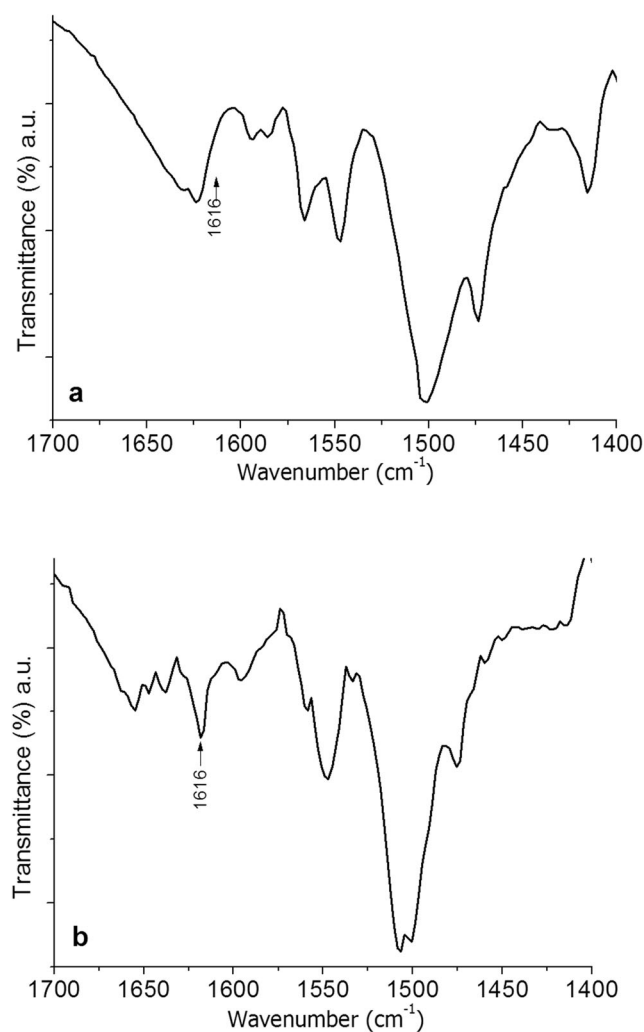
Figure 8 depicts the square wave voltammograms of two commercial samples (a) "yellow" powder food dye under anodic scan and (b) "blue" powder food dye under cathodic scan (colorful lines refer to standards and black lines to samples).

It is possible to observe that an intense peak at around − 0.15 V in Fig. 8a was present characterizing the presence of azo compounds. The sample can be characterized as tartrazine yellow due to the absence of the diagnostic peaks at − 0.8 V and its shoulder at + 0.10 V. The voltammetric profile of the standard tartrazine yellow (pink line) overlapped to the sample, perfectly matches with that observed for the yellow commercial powder (black line), being the anodic scan enough to characterize the sample. In addition, this result is in accordance with the product label stated by the manufacturer.

For characterization of the "blue" commercial sample, the cathodic scan was used and as showed in Fig. 8b, the sample present cathodic peaks at around + 1.0, + 0.6, + 0.3, − 0.35, and − 0.8 V (black line). According to the qualitative

Fig. 6 FTIR spectra from 900 to 1500 cm^{-1} of sunset yellow dye in solid state **a** before and **b** after electrolysis at + 1.3 V for 30 s

Fig. 7 FTIR spectra from 1400 to 1700 cm^{-1} of sunset yellow dye in solid state **a** before and **b** after electrolysis at − 1.3 V for 30 s

diagnostic criteria using cathodic scan, the E_{pc} at around + 1.0 V can be attributed to the presence of brilliant blue. Complementary, the sample also presented other two cathodic processes that can be attributed to this dye at around + 0.3 and − 0.8 V. In addition, Fig. 4 shows that during cathodic scan, the signals at + 0.6 and − 0.35 V can be characterized as indigotine. Thus, it is possible to infer that the sample presented both dyes in its composition and as described in the product label, both compounds were declared by the manufacturer.

The "black," "green," and "pink" food dye samples were also evaluated, and for these matrices, both anodic and cathodic scans must be used, since a mix of the dyes is applied to achieve the desired color and final composition of such samples. The use of only one scan may not be enough to identify and confirm the presence of specific dyes.

Figure 9 depicts the square wave voltammograms of (a) anodic and (b) cathodic scan of "black" sample, (c) anodic and (d) cathodic scan of "green" sample, and (e) anodic and (f) cathodic scan of "pink" sample.

As it can be observed in Fig. 9a, the anodic scan voltammetric profile of "black" food dye presented signals at around − 1.0, − 0.70, − 0.45, − 0.15, and + 0.9 V, and according to the proposed qualitative criteria, the anodic processes at − 0.70, − 0.45, and − 0.15 V can be attributed to brilliant blue, indigotine, and azo compounds, respectively. Moreover, the intense anodic peak at around + 0.9 V could also be an indicative of erythrosine; however, it is not a common dye used for green color. When cathodic scan was performed (Fig. 9b), an intense cathodic process at around + 1.0 V characterized as brilliant blue was observed. Moreover, even with a signal at around − 0.35 V characteristic of indigotine, an intense peak at around + 0.6 V was missing in the sample leading to a non-confirmation of indigotine dye. The peaks for characterization of sunset yellow was also absent during cathodic scan, leading to the presence of tartrazine yellow from the azo group dyes. This was also confirmed by the absence of the signals at around − 0.8 V and a shoulder at + 0.1 V (anodic scan) features of sunset yellow voltammetric profile.

The anodic scan shown in Fig. 9c depicted the overlapped processes from "green" food dye sample between − 0.9 and − 0.6 V besides three anodic peaks at around − 0.15, + 0.6, and + 1.0 V. A less intense peak at around − 0.45 V was also observed. The two anodic peaks between + 0.45 and + 1.2 can be features of erythrosine, brilliant blue, and indigotine. In the same way, the presence of an intense peak at around − 0.15 V is characterized as azo compounds, but the absence of a shoulder next to this intense peak rules out the presence of sunset yellow and confirm the presence of tartrazine yellow. During cathodic scan (Fig. 9d), the suspicion of erythrosine and brilliant blue was discarded by the absent of the characterization peaks at around + 0.73, + 0.40, and + 1.0, while

indigotine was confirmed by the presence of an intense peak at + 0.60 and − 0.35 V. The presences of these compounds are in accordance with the list of ingredients on the product label.

In Fig. 9e, the voltammetric profile of "pink" food dye sample presented overlapped processes from − 0.5 to − 0.15 V, a peak at + 0.5 V followed by an intense anodic peak at + 0.9 V which could be attributed to brilliant blue, indigotine, or erythrosine. However, during cathodic scan (Fig. 9f), it is possible to confirm only erythrosine due to
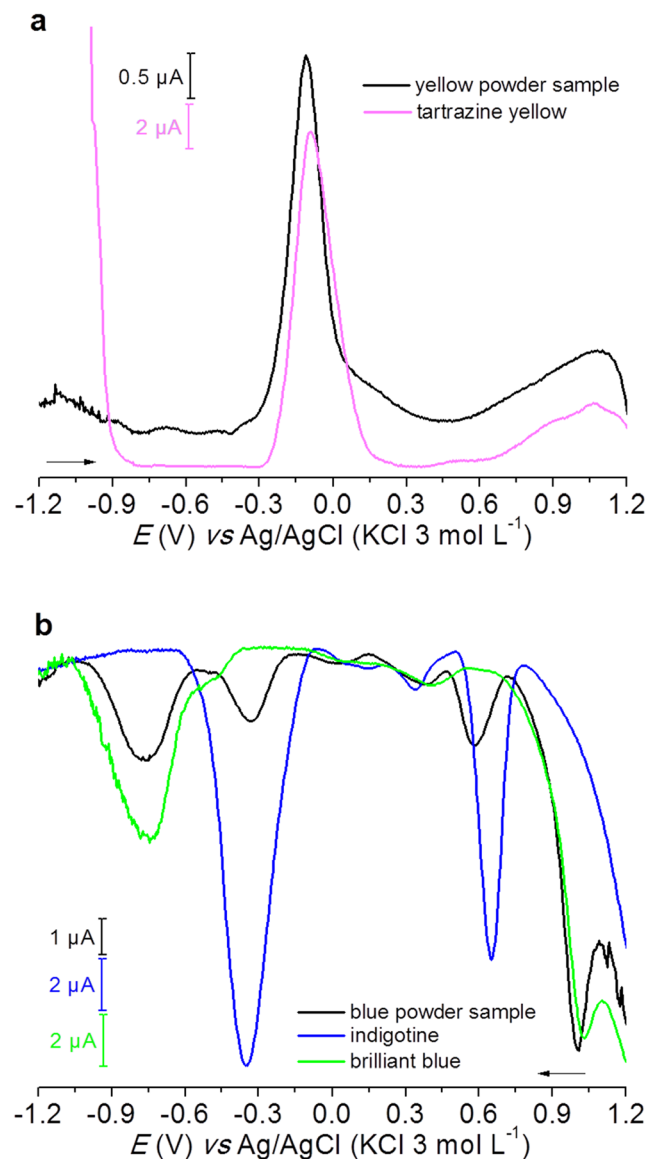
Fig. 8 Square wave voltammograms of microparticles immobilized of **a** yellow commercial powder of food dye (black line) and the standard tartrazine yellow (pink line); **b** blue commercial powder of food dye (black line), standard indigotine (blue line), and brilliant blue (green line) on the graphite electrode in NaCl 0.1 mol L^{-1} during anodic and cathodic scan, respectively. Square wave voltammetric parameters: E_{begin} − 1.2 V, E_{final} 1.2 V, E_{step} 4 mV, frequency 5 Hz, and amplitude 25 mV

the presence of two intense signals at around + 0.73 and + 0.40 V and the absence of the brilliant blue and indigotine peaks based on the qualitative diagnostic criteria depicted in Fig. 4. In addition, this dye was present in the list of ingredients on the product label.

Conclusions

Voltammetry of immobilized microparticles was used as electrochemical approach for screening of food dyes in solid state. The five dyes evaluated presented well-defined voltammetric response in solid state using NaCl 0.1 mol L^{-1} as supporting electrolyte. It was also possible

to identify and elucidate electrochemical pathways associated to the mechanisms of oxi/reduction by VIMP with special attention to sunset yellow case. A qualitative diagnostic criterion was achieved using square wave voltammetry in both anodic and cathodic scans generating different peaks for the compounds that allowed the identification and discrimination of the dyes. The criteria were suitable for screening purposes and it was applied to real samples, such as commercial powder food dyes in solid state without prior sample pretreatment. In this way, VIMP as screening method can be used as a tool for qualitative quality control, based on identification and discrimination of compounds leading only suspicious samples to more laborious and expensive analysis, such as chromatography.

Fig. 9 Square wave voltammograms of **a** anodic and **b** cathodic scans of black commercial powder of food dye (black line), tartrazine yellow, indigotine, and brilliant blue standards (pink, blue, and green lines, respectively); **c** anodic and **d** cathodic scans of green commercial powder of food dye (black line) and the standards of indigotine (blue line), brilliant blue (green line), tartrazine yellow (pink line), and erythrosine (red line); **e** anodic and **f** cathodic scans of pink commercial powder of food dye (black line) and the standards of indigotine (blue line), brilliant blue (green line), and erythrosine (red line). The solid microparticles were immobilized on the graphite electrode and immersed in NaCl 0.1 mol L^{-1}. Square wave voltammetric parameters: E_{begin} − 1.2 V, E_{final} 1.2 V, E_{step} 4 mV, frequency 5 Hz, and amplitude 25 mV

References
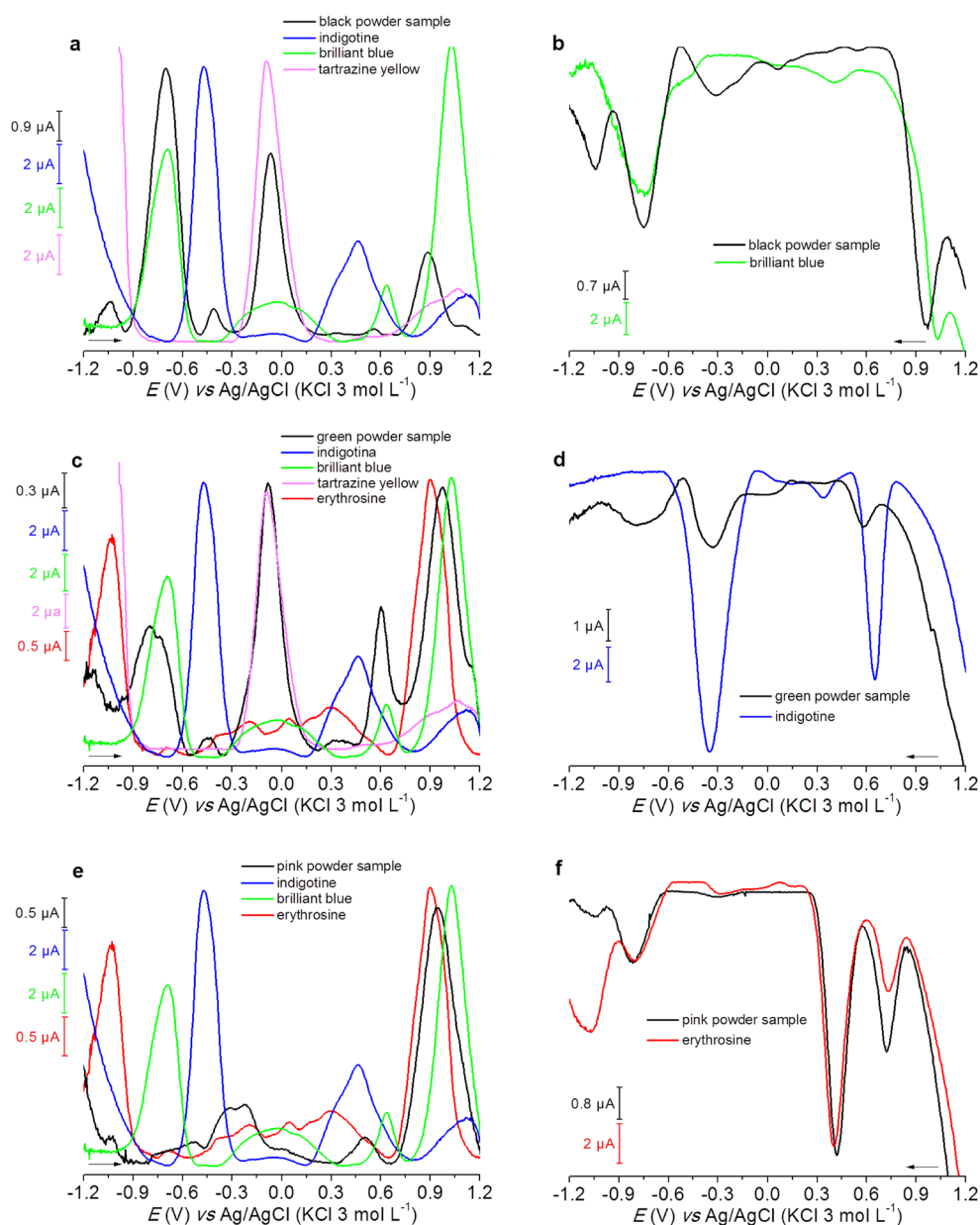
1. Kobylewski S, Jacobson MF (2012) Toxicology of food dyes. Int J Occup Environ Health 18(3):220–246. https://doi.org/10.1179/1077352512Z.00000000034

2. Stoforos NG (2015) Handbook of food processing. CRC Press, Boca Raton

3. Zhao X, Hu W, Wang Y, Zhu L, Yang L, Sha Z, Zhang J (2018) Decoration of graphene with 2-aminoethanethiol functionalized gold nanoparticles for molecular imprinted sensing of erythrosine. Carbon 127:618–626. https://doi.org/10.1016/j.carbon.2017.11.041

4. Council Directive 94/36/EC of 30 June 1994 on colours for use in foodstuffs Official Journal (1994) European Parliament, Brussels. https://eur-lex.europa.eu/legal-content/EN/ALL/?uri=celex:31994L0036.

5. Resolução n° 388 (1999) Agência Nacional de Vigilância Sanitária (ANVISA), Brasil http://portal.anvisa.gov.br/documents/33916/391619/RESOLUCAO_388_1999.pdf/ac1c03bc-17b8-46a1-b8e5-1003d3a930d8.

6. Code of Federal Regulations: Color Additives Listed for Use in Food (2015) Food and Drug Administration, Maryland. https://www.fda.gov/industry/color-additive-inventories/summary-color-additives-use-united-states-foods-drugs-cosmetics-and-medical-devices.

7. Amchova P, Kotolova H, Ruda-Kucerova J (2015) Health safety issues of synthetic food colorants. Regul Toxicol Pharmacol 73(3):914–922. https://doi.org/10.1016/j.yrtph.2015.09.026

8. Faraji M (2019) Determination of some red dyes in food samples using a hydrophobic deep eutectic solvent-based vortex assisted dispersive liquid-liquid microextraction coupled with high performance liquid chromatography. J Chromatogr A 1591:15–23. https://doi.org/10.1016/j.chroma.2019.01.022

9. Floriano L, Ribeiro LC, Saibt N, Bandeira NMG, Prestes OD, Zanella R (2018) Determination of six synthetic dyes in sports drinks by dispersive solid-phase extraction and HPLC-UV-Vis. J Braz Chem Soc. https://doi.org/10.21577/0103-5053.20170173

10. Krug FJ (2010) Métodos de preparo de amostras: fundamentos sobre o preparo de amostras orgânicas e inorgânicas para análise elementar. EditSBQ, São Paulo

11. Doménech-Carbó A, Doménech-Carbó MT, Calisti M, Maiolo V (2010) Sequential identification of organic dyes using the voltammetry of microparticles approach. Talanta. 81(1-2):404–411. https://doi.org/10.1016/j.talanta.2009.12.016

12. Martínez-Lázaro I, Doménech-Carbó A, Doménech-Carbó MT, Pastor-Valls MT, Amigó-Borrás V (2010) Electrochemical criteria for evaluating conservative treatments applied to contemporary metallic sculpture. A case study. J Solid State Electrochem 14(3):437–447. https://doi.org/10.1007/s10008-009-0908-0

13. Scholz F, Nitschke L, Henrion G, Damaschun F (1989) Abrasive stripping voltammetry - the electrochemical spectroscopy for solid state: application for mineral analysis. Fresenius' Zeitschrift Für Anal Chemie 335(2):189–194. https://doi.org/10.1007/BF00522248

14. Scholz F, Schröder U, Gulaboski R (2015) Electrochemistry of immobilized particles and droplets. Springer, Berlin

15. Komorsky-Lovrić Š, Scholz F (1998) Stripping chronopotentiometry of immobilized microparticles. J Electroanal Chem 445(1-2):81–87. https://doi.org/10.1016/S0022-0728(97)00569-X

16. Maciel JV, Fava EL, Silva TA, Dias D, Fatibello-Filho O (2017) A combination of voltammetry of immobilized microparticles and carbon black-based crosslinked chitosan films deposited on glassy carbon electrode for the quantification of hydroquinone in dermatologic cream samples. J Solid State Electrochem 21(10):2859–2868. https://doi.org/10.1007/s10008-017-3614-3

17. Maciel JV, Silva TA, Dias D, Fatibello-Filho O (2018) Electroanalytical determination of eugenol in clove oil by voltammetry of immobilized microdroplets. J Solid State Electrochem 22(7):2277–2285. https://doi.org/10.1007/s10008-018-3933-z

18. Martini M, Machado De Carvalho L, Blasco-Blasco A, Doménech-Carbó A (2015) Screening and authentication of herbal formulations based on microextraction-assisted voltammetry of microparticles. Anal Methods 7(14):5740–5747. https://doi.org/10.1039/c5ay01145k

19. Doménech-Carbó A, De Carvalho LM, Martini M, Cebrián-Torrejón G (2014) Voltammetric/amperometric screening of compounds of pharmacological interest. Rev Anal Chem 33(3). https://doi.org/10.1515/revac-2013-0027

20. Doménech-Carbó A, da Silveira GD, Medina-Alcaide MÁ, Carmona AM, López-Serrano D, Pasíes-Oviedo T, Algarra-Pardo VM, de Carvalho LM, Montoya N (2018) Polythiophenes as markers of asphalt and archaeological tar pitch aging. Characterization using solid-state electrochemistry. Electrochem Commun 87:18–21. https://doi.org/10.1016/j.elecom.2017.12.020

21. Doménech-Carbó A, Doménech-Carbó MT, Pascual MLVA (2006) Dehydroindigo: a new piece into the Maya Blue puzzle from the voltammetry of microparticles approach. J Phys Chem B 110(12):6027–6039. https://doi.org/10.1021/jp057301l

22. Doménech-Carbó A, Martini M, De Carvalho LMH, Doménech-Carbó MT (2012) Square wave voltammetric determination of the redox state of a reversibly oxidized/reduced depolarizer in solution and in solid state. J Electroanal Chem 684:13–19. https://doi.org/10.1016/j.jelechem.2012.08.016

23. Doménech-Carbó A, Doménech-Carbó MT, Pascual MLVA (2007) Chemometric study of Maya Blue from the voltammetry of microparticles approach. Anal Chem 79(7):2812–2821. https://doi.org/10.1021/ac0623686

24. Grygar T, Kučková Š, Hradil D, Hradilová J (2003) Electrochemical analysis of natural solid organic dyes and pigments. J Solid State Electrochem 7(10):706–713. https://doi.org/10.1007/s10008-003-0380-1

25. Doménech-Carbó A, Doménech-Carbó MT, Saurí-Peris MC, Gimeno-Adelantado JV, Bosch-Reig F (2003) Electrochemical identification of anthraquinone-based dyes in solid microsamples by square wave voltammetry using graphite/polyester composite electrodes. Anal Bioanal Chem 375(8):1169–1175. https://doi.org/10.1007/s00216-002-1742-8

26. Lovrić M, Scholz F (1997) A model for the propagation of a redox reaction through microcrystals. J Solid State Electrochem 1(1):108–113. https://doi.org/10.1007/s100080050030

27. Doménech-Carbó A, Dias D, Doménech-Carbó MT (2020) Cation and anion electrochemically assisted solid-state transformations of malachite green. Phys Chem Chem Phys 22(3):1502–1510. https://doi.org/10.1039/c9cp05835d

28. Doménech-Carbó A (2012) Solvent-independent electrode potentials of solids undergoing insertion electrochemical reactions: Part I. theory. J Phys Chem C. https://doi.org/10.1021/jp308966w

29. Doménech-Carbó A, Labuda J, Scholz F (2013) Electroanalytical chemistry for the analysis of solids: characterization and classification (IUPAC technical report). Pure Appl Chem 85(3):609–631. https://doi.org/10.1351/PAC-REP-11-11-13

30. Scholz F, Doménech-Carbó A (2019) The thermodynamics of insertion electrochemical electrodes - a team play of electrons and ions across two separate interfaces. Angew Chem Int Ed 58(11): 3279–3284. https://doi.org/10.1002/anie.201809631

31. Doménech-Carbó A, Doménech-Carbó MT (2006) Chronoamperometric study of proton transfer/electron transfer in solid state electrochemistry of organic dyes. J Solid State Electrochem 10(12):949–958. https://doi.org/10.1007/s10008-005-0018-6

32. Doménech A, Doménech-Carbó MT, de Agredos Pascual MLV (2007) Electrochemical monitoring of indigo preparation using Maya's ancient procedures. J Solid State Electrochem 11(9): 1335–1346. https://doi.org/10.1007/s10008-007-0296-2

33. Doménech A, Doménech-Carbó MT, del Río MS, de Agredos Pascual MLV (2009) Comparative study of different indigo-clay Maya Blue-like systems using the voltammetry of microparticles approach. J Solid State Electrochem 13(6):869–878. https://doi.org/10.1007/s10008-008-0616-1

34. Yamjala K, Nainar MS, Ramisetti NR (2016) Methods for the analysis of azo dyes employed in food industry - a review. Food Chem 192:813–824. https://doi.org/10.1016/j.foodchem.2015.07.085

35. Vladislavić N, Buzuk M, Rončević IS, Brinić S (2018) Electroanalytical methods for determination of sunset yellow - a review. Int J Electrochem Sci. https://doi.org/10.20964/2018.07.39

36. Ahmad I, Murtaza S, Ahmed S (2015) Electrochemical and photovoltaic study of sunset yellow and tartrazine dyes. Monatsh Chem 146(10):1631–1640. https://doi.org/10.1007/s00706-015-1425-8

37. Yu J, Jia J, Ma Z (2004) Comparison of electrochemical behavior of hydroxyl-substituted and nonhydroxyl-substituted azo dyes at a glassy carbon electrode. J Chin Chem Soc 51(6):1319–1324. https://doi.org/10.1002/jccs.200400191

38. Carey FA (2008) Organic chemistry. AMGH, New York

39. da Silveira GD, de Carvalho LM, Montoya N, Domenech-Carbó A (2017) Solid state electrochemical behavior of organosulfur compounds. J Electroanal Chem 806:180–190. https://doi.org/10.1016/j.jelechem.2017.10.055

40. Socrates G (2001) Infrared and Raman characteristic group frequencies. Wiley, Middlesex

41. da Silveira GD, Bressan LP, Schmidt MEP, Dal Molin TR, Teixeira CA, Poppi RJ, da Silva JAF (2020) Electrochemical behavior of 5-type phosphodiesterase inhibitory drugs in solid state by voltammetry of immobilized microparticles. J Solid State Electrochem. https://doi.org/10.1007/s10008-020-04533-1

Publisher's note Springer Nature remains neutral with regard to jurisdictional claims in published maps and institutional affiliations.